# A STOCHASTIC COLLOCATION METHOD BASED ON SPARSE GRIDS FOR A STOCHASTIC STOKES-DARCY MODEL

### ZHIPENG YANG

Division of Applied and Computational Mathematics Beijing Computational Science Research Center Beijing 100094, China

### XUEJIAN LI AND XIAOMING HE

Department of Mathematics and Statistics Missouri University of Science and Technology Rolla, MO 65409, USA

### Ju Ming\*

School of Mathematics and Statistics Huazhong University of Science and Technology Wuhan 430074, China

ABSTRACT. In this paper, we develop a sparse grid stochastic collocation method to improve the computational efficiency in handling the steady Stokes-Darcy model with random hydraulic conductivity. To represent the random hydraulic conductivity, the truncated Karhunen-Loève expansion is used. For the discrete form in probability space, we adopt the stochastic collocation method and then use the Smolyak sparse grid method to improve the efficiency. For the uncoupled deterministic subproblems at collocation nodes, we apply the general coupled finite element method. Numerical experiment results are presented to illustrate the features of this method, such as the sample size, convergence, and randomness transmission through the interface.

1. **Introduction.** The Stokes-Darcy (SD) model is a fundamental model used in many areas of science and engineering, for example, groundwater systems in karst aquifers [25, 49, 60, 61], interaction between surface and subsurface flows [28, 36, 38, 66, 75], oil reservoir in vuggy porous medium [1, 3, 41, 84, 120], and industrial filtrations [44,62]. The Stokes-Darcy model describes the free flow of a liquid by the Stokes equation and the confined flow in a porous media by the Darcy equation, the two flows are coupled through interface conditions. Due to the fact that the resulting coupled Stokes-Darcy model has higher fidelity than either the Darcy or Stokes systems on their own, it is not surprising that a great deal of effort has been devoted to developing numerical methods for solving the model, such as the coupled finite element methods [21,72,85,99], domain decomposition methods [19,24,31,37,39,40,57,79,108], Lagrange multiplier methods [6,50,76], multi-grid methods [2,20,88],

1

 $<sup>2020\</sup> Mathematics\ Subject\ Classification.\ 76S05,\ 35R60,\ 65D40,\ 65N35,\ 65M60.$ 

Key words and phrases. Stokes-Darcy flow, stochastic partial differential equation, Karhunen-Loève expansion, sparse grid, stochastic collocation method, finite elements.

This work is partially supported by NSF grant DMS-1722647.

<sup>\*</sup> Corresponding author: Ju Ming.

discontinuous Galerkin methods [33,54,71,78,96], mortar discretization [17,48,55], and many others [5,10,18,22,32,43,63,68,70,77,83,89,100,110,111,119].

All of the above existing work focused on the deterministic SD model, in which the model parameters, such as the model coefficients, the forcing terms, the domain geometry, the boundary conditions, the initial conditions, etc., are assumed to be perfectly known. Rather surprisingly, there are only limited number of literature studies about the stochastic SD model [74]. In reality, there is a huge amount of uncertainty involved in determining these real-life data due to measurement noise and simplifications. Hence many applications are affected by a relatively large amount of uncertainty in the input data, which cannot be accurately modeled by deterministic partial differential equations. On the other hand, modern engineering relies more and more on computational simulations, and the accuracy requirement in the computational results is growing significantly.

There are many sources that could generate uncertainties in SD model, which may come from either our difficulty in characterizing the investigated complex system or an intrinsic variability of physical quantities. For instance, when we study subsurface flows, the subsurface properties, such as porosity and permeability, are usually extrapolated from measurements taken in a limited number of sampling locations. When enough information is provided for the statistical characterization of the physical system, the input data can be modeled as random fields with a given correlation structure in associated PDEs, see e.g, the Karhunen-Loève [80,81] and polynomial chaos expansions [116,117]. Then instead of determining a single solution, we are concerned with the statistical moments of the solutions, such as their mean value, variance, covariance, i.e., the derived statistical quantities of interests.

A number of efficient numerical methods have been developed to solve stochastic PDEs, such as polynomial chaos [69,116,117], stochastic Galerkin method [8,35,86,98], stochastic collocation method [7,59], sparse grid methods [11,87,90,91], multilevel Monte Carlo method [14,29,42,52,73,97,104], and many others [9,12,27,82,103,107,109,112,114,115,118,121,122]. These methods have also been applied to solve the stochastic optimization and control problems [4,13,34,58,105].

Similar to the Monte Carlo method [46], the stochastic collocation method [7] is characterized by requiring only the solution of uncoupled deterministic problems over the set of collocation points, even in the presence of a hydraulic conductivity which depends nonlinearly on the random variables. That is, the stochastic collocation method is naturally parallel with minimum communication and capable of fully making use of existing packages as black boxes for the corresponding deterministic problems. However, the stochastic collocation method with full tensor product spaces still suffers from the so-called *curse of dimensionality*(COD) when high-dimensional random variables are needed to describe the input data.

Meanwhile, the sparse grid method [15,51,102] is an efficient technique to avoid the dilemma caused by COD due to its selection of quadrature points based on their estimated contributions to the numerical quadrature's overall accuracy. When the dimension is moderately large and when the integrand depends smoothly on the underlying random variables, the advantage of sparse grid becomes more clear as the increase of the number of dimensions.

In this article, we will follow the idea in [90,91] to develop a sparse grid stochastic collocation method for a Stokes-Darcy model with random hydraulic conductivity, which is described by a finite-dimensional random vector. As pointed out in [90,91], this is often called finite-dimensional noise assumption and may hold either because

the problem itself can be described by a finite number of random variables or because the input coefficients are modeled as truncated random fields.

The rest of paper is organized as follows. In section 2, we introduce the Stokes-Darcy system with random hydraulic conductivity. In section 3, we treat the random hydraulic conductivity by using Karhunen-Loève expansion to obtain the truncated stochastic Stokes-Darcy model. In section 4, a Smolyak based sparse grid method is proposed to solve the truncated stochastic Stokes-Darcy model. Finally, in section 6, we present some numerical results that illustrate the features of the proposed method.

2. Steady Stokes-Darcy model with random hydraulic conductivity. We consider the coupled Stokes-Darcy system on a bounded domain  $\Omega = \Omega_D \cup \Omega_S \subset \mathbb{R}^d$ , (d = 2, 3); see Figure 1. Assume  $(\Omega_P, \mathcal{F}, \mathcal{P})$  is a complete probability space.

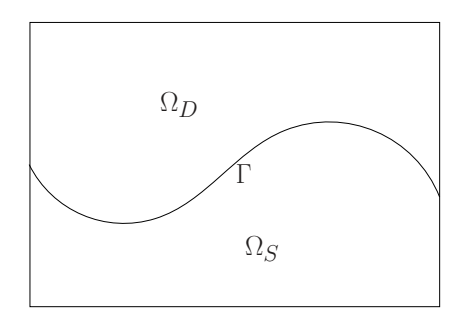


FIGURE 1. A sketch of the porous media domain  $\Omega_D$ , the free-flow domain  $\Omega_S$ , and the interface  $\Gamma$ .

Here  $\Omega_P$  is the set of outcomes,  $\mathcal{F}$  is the  $\sigma$ -algebra of events, and  $\mathcal{P}: \mathcal{F} \to [0,1]$  is a probability measure. In the porous media region  $\Omega_D$ , the flow is governed by the Darcy system

$$\vec{u}_D(\omega, x) = -K(\omega, x)\nabla\phi_D(\omega, x),$$
 (1)

$$\nabla \cdot \vec{u}_D(\omega, x) = f_D. \tag{2}$$

where  $\omega \in \Omega_P, x \in \Omega_D$ . Here,  $\vec{u}_D$  is the fluid discharge rate in the porous media, K is the random hydraulic conductivity,  $f_D$  is a sink/source term, and  $\phi_D$  is the hydraulic head defined as  $\phi_D = z + \frac{p_D}{\rho g}$ . Here  $p_D$  denotes the dynamic pressure, z denotes the height,  $\rho$  denotes the density, and g denotes the gravitational acceleration. In this article we will consider the the second-order form of the Darcy system

$$-\nabla \cdot (K(\omega, x)\nabla \phi_D(\omega, x)) = f_D. \tag{3}$$

In the fluid region  $\Omega_S$ , the fluid flow is assumed to satisfy the Stokes system

$$-\nabla \cdot \mathbb{T}(\vec{u}_S, p_S) = \vec{f}_S, \tag{4}$$

$$\nabla \cdot \vec{u}_S = 0, \tag{5}$$

where  $\vec{u}_S$  is the fluid velocity,  $p_S$  is the kinematic pressure,  $\vec{f}_S = (\vec{f}_{S1}, \vec{f}_{S2})$  is the external body force,  $\nu$  is the kinematic viscosity of the fluid,  $\mathbb{T}(\vec{u}_S, p_S) = 2\nu \mathbb{D}(\vec{u}_S) - p_S \mathbb{I}$  is the stress tensor, and  $\mathbb{D}(\vec{u}_S) = 1/2(\nabla \vec{u}_S + \nabla^\top \vec{u}_S)$  is the deformation tensor.

Let  $\Gamma = \overline{\Omega}_D \cap \overline{\Omega}_S$  denote the interface between the fluid and porous media regions. On  $\Gamma$ , we consider the following three interface conditions which are also affected by the randomness of the hydraulic conductivity K:

$$\vec{u}_S \cdot \vec{n}_S = -\vec{u}_D \cdot \vec{n}_D, \tag{6}$$

$$-\vec{n}_S \cdot (\mathbb{T}(\vec{u}_S, p_S) \cdot \vec{n}_S) = g(\phi_D - z), \tag{7}$$

$$-\boldsymbol{\tau}_{j} \cdot (\mathbb{T}(\vec{u}_{S}, p_{S}) \cdot \vec{n}_{S}) = \frac{\alpha \nu \sqrt{\mathbf{d}}}{\sqrt{\operatorname{trace}(\prod)}} \boldsymbol{\tau}_{j} \cdot (\vec{u}_{S} - \vec{u}_{D}), \tag{8}$$

where  $\vec{n}_S$  and  $\vec{n}_D$  denote the unit outer normal to the fluid and the porous media regions at the interface  $\Gamma$ , respectively;  $\tau_j$   $(j=1,\ldots,d-1)$  denote mutually orthogonal unit tangential vectors to the interface  $\Gamma$ , and  $\prod(\omega,x)=\frac{K(\omega,x)\nu}{g}$ . The third condition (8) is referred as the Beavers-Joseph (BJ) interface condition [16, 23, 25, 26, 45, 64, 67, 95, 101]. Compared with the Beavers-Joseph-Saffman-Jones (BJSJ) interface boundary condition [76], the Beavers-Joseph interface condition considers the contribution of the flow in the porous media to the tangential interface condition. More theoretical support for the BJ condition can be found in [30], which demonstrated that the BJ condition is more accurate than the BJSJ condition or its further simplifications.

We also assume that the hydraulic head  $\phi_D$  and the fluid velocity  $\vec{u}_S$  satisfy homogeneous Dirichlet boundary condition except on  $\Gamma$ , i.e.,  $\phi_D=0$  on the boundary  $\partial\Omega_D\backslash\Gamma$  and  $\vec{u}_S=0$  on the boundary  $\partial\Omega_S\backslash\Gamma$ . We also assume that  $K(\omega,\cdot)$  is uniformly bounded below, i.e., there exists a constant  $K_0>0$  such that  $P(\omega\in\Omega_P:K(\omega,x)>K_0,x\in\overline{\Omega}_D)=1$ .

3. Karhunen-Loève expansion and truncated stochastic Stokes-Darcy model. In this section, we will recall the Karhunen-Loève (KL) expansion [80,81] for a positive random field  $r(\omega, x)$ , with continuous covariance function  $\text{Cov}_r(x, x')$ :  $\Omega_D \times \Omega_D \to \mathbb{R}$ , and then utilize the truncated KL expansion to obtain the truncated stochastic Stokes-Darcy model.

We first consider the following eigenvalue problem:

$$\int_{\Omega_{\mathcal{D}}} \operatorname{Cov}_{r}(x, x') v(x') dx' = \lambda v(x). \tag{9}$$

Due to the symmetry of  $\operatorname{Cov}_r(\cdot,\cdot)$  and the positivity of  $r(\omega,x)$ , the eigenvalues  $\{\lambda_n\}_{n=1}^{\infty}$  are real and nonnegative, and the eigenspace span $\{v_1,v_2,\cdots,v_n,\cdots\}$  corresponding to distinct eigenvalues is mutually orthogonal, i.e.,

$$\int_{\Omega_D} v_m(x)v_n(x)dx = \delta_{mn}, \ \forall \ m, n \in \mathbb{N}^+.$$
 (10)

Since the eigenvalues are nonnegative, we may order the eigenvalues  $\{\lambda_n\}_{n=1}^{\infty}$  as  $\lambda_1 \geq \lambda_2 \geq \lambda_3 \geq \cdots \geq 0$ . Let  $\mu_r(x)$  denote the expected value of  $r(\omega, x)$ . Define

$$Y_n(\omega) = \frac{1}{\sqrt{\lambda_n}} \int_{\Omega_D} \left[ r(\omega, x) - \mu_r(x) \right] v_n(x) dx. \tag{11}$$

Here  $\{Y_n(\omega)\}_{n=1}^{\infty}$  are mutually uncorrelated real random variables with zero mean and unit variance, i.e.,  $\mathbb{E}(Y_n(\omega)) = 0$ ,  $\mathbb{E}(Y_m(\omega)Y_n(\omega)) = \delta_{mn}$ . Then the KL expansion is defined by

$$r(\omega, x) = \mu_r(x) + \sum_{n=1}^{\infty} \sqrt{\lambda_n} v_n(x) Y_n(\omega).$$
 (12)

The validity of the KL expansion results from the fact that the eigenvalues  $\{\lambda_n\}_{n=1}^{\infty}$  decay as n increases. The decay rate depends on the smoothness of the covariance function  $\text{Cov}_r(x,x')$  and the correlation length, see [47,106] and references therein. Based on the desired accuracy, we may retain only the first N terms to obtain the following truncated KL expansion

$$r_N(\omega, x) = \mu_r(x) + \sum_{n=1}^N \sqrt{\lambda_n} v_n(x) Y_n(\omega), \ \forall \ N \in \mathbb{N}^+.$$
 (13)

Using a KL representation of random fields, we consider the following problem instead of (3).

$$-\nabla \cdot (K_N(\omega, x)\nabla \phi_N(\omega, x)) = f_D. \tag{14}$$

One important issue is the elliptic coercivity of  $K_N(\omega, x)$ . One often performs a truncated Karhunen-Loève expansion for  $\log(K - K_{min})$  instead of K to obtain

$$\log(K_N - K_{min})(\omega, x) = \mu(x) + \sum_{n=1}^N \sqrt{\lambda_n} v_n(x) Y_n(\omega), \ \forall \ N \in \mathbb{N}^+.$$
 (15)

Here  $K(\omega, x) \geq K_{min}, \ \forall \ x \in \Omega_D$ . Then we have

$$K_N(\omega, x) = K_{min} + e^{\mu(x) + \sum_{n=1}^N \sqrt{\lambda_n} v_n(x) Y_n(\omega)}, \ \forall \ N \in \mathbb{N}^+.$$
 (16)

In this article, we assume  $Y_n(\omega)$  to be bounded, denote the image of  $Y_n$  by  $I_n = Y_n(\Omega_P)$ , and define  $\mathbf{I}^N = \prod_{n=1}^N I_n$ . Also, we assume that the random variables  $\{Y_n\}_{n=1}^N$  have a joint probability density function  $\rho_Y: \mathbf{I}^N \to \mathbb{R}^+$  such that  $\rho_Y \in L^{\infty}(\mathbf{I}^N)$ . Hence in the rest of this article, we consider the following problem

$$-\nabla \cdot (K_N(\omega, x)\nabla \phi_N(\omega, x)) = f_D, \tag{17}$$

$$-\nabla \cdot \mathbb{T}(\vec{u}_N(\omega, x), p_N(\omega, x)) = \vec{f}_S, \tag{18}$$

$$\nabla \cdot \vec{u}_N(\omega, x) = 0, \tag{19}$$

$$\vec{u}_N(\omega, x) \cdot \vec{n}_S = K_N(\omega, x) \nabla \phi_N(\omega, x) \cdot \vec{n}_D,$$
 (20)

$$-\vec{n}_S \cdot (\mathbb{T}(\vec{u}_N(\omega, x), p_N(\omega, x)) \cdot \vec{n}_S) = g(\phi_N(\omega, x) - z), \tag{21}$$

$$-\boldsymbol{\tau}_{j} \cdot (\mathbb{T}(\vec{u}_{N}(\omega, x), p_{N}(\omega, x)) \cdot \vec{n}_{S}) = \frac{\alpha \nu \sqrt{\mathbf{d}}}{\sqrt{\operatorname{trace}(\prod_{N})}} \boldsymbol{\tau}_{j} \cdot (\vec{u}_{N}(\omega, x) + K_{N}(\omega, x) \nabla \phi_{N}(\omega, x)), \qquad (22)$$

where  $\prod_{N}(\omega, x) = \frac{K_N(\omega, x)\nu}{q}$ .

4. Sparse grid stochastic collocation method for the Stokes-Darcy model. In this section, we present the sparse grid stochastic collocation method for the Stokes-Darcy model (17) -(21) with Beavers-Joseph (BJ) interface condition (22), where the random hydraulic conductivity  $K(\omega, x)$  is represented by the truncated Karhunen-Loève expansion (16).

We first apply the stochastic collocation method to construct the discrete form in probability, and then use the sparse grid method to reduce the computational cost. To solve the deterministic Stokes-Darcy model at each collocation node (i.e., for each sample), we adopt the regular coupled finite element method (FEM).

4.1. Stochastic collocation method. Define a multi-index  $\vec{p} = (p_1, p_2, \dots, p_N)$ ,  $|\vec{p}| = \sum_{n=1}^{N} p_n$ ,

$$P_{p_n}(I_n) = \text{span}\{y_n^k, k = 0, \dots, p_n\}, \ n = 1, \dots, N,$$
 (23)

$$\mathbf{P}_{\vec{p}}(\mathbf{I}^N) = \bigotimes_{n=1}^N \mathbf{P}_{p_n}(\mathbf{I}_n) \subset L^2_{\rho_Y}(\mathbf{I}^N). \tag{24}$$

For stochastic PDEs, one is often interested in determining statistical information about the quantities of interest, given statistical information about the inputs. For the stochastic Stokes-Darcy model, we design a numerical method to calculate the moments for determining statistical information about the quantities of interests. To construct the discrete form in the probability space, we choose a set of collocation points  $\{\vec{y}_i\}_{i=1}^M \subset \mathbf{I}^N$  and a set of polynomials  $\{l_k^{\vec{p}}(\vec{y})\}_{i=1}^M \subset \mathbf{P}_{\vec{p}}(\mathbf{I}^N)$  correspondingly, such as Lagrange polynomials. Then the discrete solutions in the probability space are

$$\phi_{N,\vec{p}}(\vec{y},x) = \sum_{i=1}^{M} \phi_N(\vec{y}_i,x) l_k^{\vec{p}}(\vec{y}), \qquad (25)$$

$$\vec{u}_{N,\vec{p}}(\vec{y}_i, x) = \sum_{i=1}^{M} \vec{u}_N(\vec{y}_i, x) l_k^{\vec{p}}(\vec{y}), \tag{26}$$

$$p_{N,\vec{p}}(\vec{y}_i, x) = \sum_{i=1}^{M} p_N(\vec{y}_i, x) l_k^{\vec{p}}(\vec{y}).$$
 (27)

For the discretization in the physical space, the finite element method (FEM) is utilized. In other words, for each  $\vec{y}_i(i=1,\cdots,M)$ ,  $\phi_N(\vec{y}_i,x)$ ,  $\vec{u}_N(\vec{y}_i,x)$  and  $p_N(\vec{y}_i,x)$  can be approximated numerically by  $\phi_{N,h}(\vec{y}_i,x)$ ,  $\vec{u}_{N,h}(\vec{y}_i,x)$  and  $p_{N,h}(\vec{y}_i,x)$  by using a deterministic discretization method in  $\Omega$ . Then the final discrete solutions are

$$\phi_{N,h,\vec{p}}(\vec{y},x) = \sum_{i=1}^{M} \phi_{N,h}(\vec{y}_i,x) l_k^{\vec{p}}(\vec{y}), \qquad (28)$$

$$\vec{u}_{N,h,\vec{p}}(\vec{y}_i,x) = \sum_{i=1}^{M} \vec{u}_{N,h}(\vec{y}_i,x) l_k^{\vec{p}}(\vec{y}),$$
 (29)

$$p_{N,h,\vec{p}}(\vec{y}_i, x) = \sum_{i=1}^{M} p_{N,h}(\vec{y}_i, x) l_k^{\vec{p}}(\vec{y}).$$
 (30)

Let  $w_k = \mathbb{E}(l_k^{\vec{p}})$ . Then the expected value of functions  $\gamma(\phi_N)$ ,  $\gamma(\vec{u}_N)$ , and  $\gamma(p_N)$  can be obtained as follows.

$$\mathbb{E}(\gamma(\phi_N)) \approx \mathbb{E}(\gamma(\phi_{N,h,\vec{p}})) \approx \sum_{i=1}^M w_i \gamma(\phi_{N,h}(\vec{y}_i, x)), \tag{31}$$

$$\mathbb{E}(\gamma(\vec{u}_N)) \approx \mathbb{E}(\gamma(\vec{u}_{N,h,\vec{p}})) \approx \sum_{i=1}^{M} w_i \gamma(\vec{u}_{N,h}(\vec{y}_i, x)), \tag{32}$$

$$\mathbb{E}(\gamma(p_N)) \approx \mathbb{E}(\gamma(p_{N,h,\vec{p}})) \approx \sum_{i=1}^{M} w_i \gamma(p_{N,h}(\vec{y}_i, x)). \tag{33}$$

Here  $w_i(i=1,\cdots,M)$  and  $\vec{y}_i(i=1,\cdots,M)$  are the weights and nodes of some numerical quadratures, such as Gauss quadratures. One regular method for choosing  $\vec{y}_i(i=1,\cdots,M)$  is the full tensor-product interpolation. Let  $x_n^{j_n}, w_n^{j_n}, j_n = 1, 2, \cdots, m_n$  be the quadrature nodes and weights over the interval  $I_n, n = 1, 2, \cdots, N$ . Here  $m_n \in \mathbb{N}$  is the number of quadrature nodes over the one dimensional interval  $I_n, n = 1, 2, \cdots, N$ . Then the full tensor-product interpolation to calculate the expected value of function  $\gamma(\phi_N)$  is given as

$$\mathbb{E}(\gamma(\phi_N)) \approx \sum_{j_1=1}^{m_1} \cdots \sum_{j_N=1}^{m_N} \left( \prod_{\ell=1}^N w_\ell^{j_\ell} \right) \gamma(\phi_{N,h}(x_1^{j_1}, \cdots, x_N^{j_N}, x)).$$
 (34)

The set of collocation nodes is given as  $\{\vec{y}_i\}_{i=1}^M = X_1 \times \cdots \times X_N \subset \mathbf{I}^N$  with  $X_n = \{x_n^1, x_n^2, \cdots, x_n^{m_n}\}, n = 1, 2, \cdots, N$ , and the total number of quadrature nodes is  $M = \prod_{n=1}^N m_n$ . When the dimension N of the truncated stochastic space becomes larger, the number M of quadrature nodes of full tensor product interpolation increases significantly. For each collocation node  $\vec{y}_i$ , we need to solve the corresponding deterministic Stokes-Darcy model one time to obtain the FEM approximations  $\phi_{N,h}(\vec{y}_i,x), \vec{u}_{N,h}(\vec{y}_i,x), p_{N,h}(\vec{y}_i,x)$ . Therefore the computational cost increases quickly when the dimension N of the truncated stochastic space becomes larger. This leads to a great need in an efficient numerical method using small number of collocation nodes to reduce the computational cost. One efficient technique to dramatically reduce this curse of dimensionality is sparse grid [15,51,102], which will be discussed in the next subsection.

4.2. Algorithm of sparse grid stochastic collocation method. Let  $w_j^{i_n}, x_j^{i_n}, j=1,2,\cdots,m_i\in\mathbb{N}$  be the weights and nodes of numerical quadrature with the accuracy level i over the one dimensional interval  $I_n, n=1,2,\cdots,N$  so that the order of polynomial exactness increases with  $i_n$ . For the numerical integral  $Q^{i_n}$  with different accuracy level  $i_n$  of the function f over the one dimensional interval  $I_n$ , the quadrature formulas are given as

$$Q^{i_n}(f) = \sum_{j=1}^{m_{i_n}} f(x_j^{i_n}) w_j^{i_n}, \quad n = 1, 2, \dots, N.$$
 (35)

For the multivariate case N > 1, we define the quadrature formula by the full tensor product interpolation as

$$(Q^{i_1} \otimes \cdots \otimes Q^{i_N})(f) = \sum_{j_1=1}^{m_{i_1}} \cdots \sum_{j_N=1}^{m_{i_N}} \left(\prod_{\ell=1}^N w_\ell^{j_\ell}\right) f(x_{j_1}^{i_1}, \cdots, x_{j_N}^{i_N}).$$
(36)

The full tensor product interpolation (36) has the accuracy level in each dimension is  $i_n, n = 1, 2, \dots, N$ .

For the multi-index  $\vec{i} = (i_1, i_2, \dots, i_N)$ , we define  $|\vec{i}| = \sum_{n=1}^{N} i_n$ . For the numerical integral  $Q^i$ , we denote

$$Q^{0} = 0, \quad \Delta^{i} = Q^{i} - Q^{i-1}, \quad i \in \mathbb{N}.$$
 (37)

Then the quadrature formula in the multivariate case N>1 by the algorithm of Smolyak [15,65,90,91,102] with accuracy level  $s\in\mathbb{N}$  to construct the sparse grid is given by

$$Q(s,N) = \sum_{\ell=0}^{s-1} \sum_{|\vec{i}|=N+\ell} \left( \Delta^{i_1} \otimes \cdots \otimes \Delta^{i_N} \right).$$
 (38)

Equivalently, the analogous formula [65,113] is

$$Q(s,N) = \sum_{\ell=s-N}^{s-1} (-1)^{s-1-\ell} {N-1 \choose s-1-\ell} \sum_{|\vec{i}|=N+\ell} (Q^{i_1} \otimes \cdots \otimes Q^{i_N}).$$
 (39)

Let  $X^i = \{x_1^i, x_2^i, \dots, x_{m_i}^i\}$  be the set of quadrature nodes for the numerical integral  $Q^i$ . Based on formula (36), the set of quadrature nodes for the full tensor numerical integral  $(Q^{i_1} \otimes \cdots \otimes Q^{i_N})$  is  $X^{i_1} \times \cdots X^{i_N}$ . And the set of quadrature nodes for the algorithm of Smolyak to construct the sparse grid in the formula (38) or (39) is

$$\mathcal{H}(s,N) = \bigcup_{\ell=s-N}^{s-1} \bigcup_{|\vec{i}|=N+\ell} \left( X^{i_1} \times \dots \times X^{i_N} \right). \tag{40}$$

There are many numerical integral methods to determine the quadrature weights and nodes over the one dimensional interval  $I_n$  for the formula (35). In this paper, we adopt the Gauss-Legendre abscissas (GQU) [15, 65, 90, 91] and Kronrod-Patterson abscissas (KPU) [65,92–94] to generate the quadrature nodes set  $X^i$  $\{x_1^i, x_2^i, \cdots, x_{m_i}^i\}$ . The quadrature nodes of the Gauss-Legendre abscissas are the roots of Legendre polynomials with the Gauss-Legendre quadrature rule. The quadrature nodes of Kronrod-Patterson abscissas are generated by the Kronrod-Patterson quadrature formula, which is a variant of Gaussian quadrature formula to derive the nested quadrature nodes. For either the Kronrod-Patterson abscissas or Gauss-Legendre abscissas, the number of the quadrature nodes in sparse grid (40) is much smaller than the number of the quadrature nodes in the full tensor product interpolation (36), since the sparse grid method is capable of attaining a high accuracy when only choosing lower level  $\vec{i}$ . Hence the computational expense is reduced significantly by the sparse grid method. We now apply the sparse grid using the Gauss-Legendre abscissas (GQU) and Kronrod-Patterson abscissas (KPU) to solve the Stokes-Darcy model (17) -(22). The details of using sparse grid method to solve the Stokes-Darcy model are given in the following Algorithm 1.

## Algorithm 1 SG-SC algorithm

**Input:** The interpolation abscissas and the sparse grid accuracy level s.

- 1: Obtain the collocation points  $\{\vec{y}_i\}_{i=1}^M$  and numerical quadrature weights  $\{w_i\}_{i=1}^M$  from the Smolyak sparse grid of GQU and KPU.
- 2: For  $i=1,\cdots,M$ , independently solve the Stokes-Darcy model (17)-(22) on each collocation point  $\vec{y_i}$ . More precisely, the finite element solutions  $\phi_{N,h}(\vec{y_i},x)$ ,  $\vec{u}_{N,h}(\vec{y_i},x)$  and  $p_{N,h}(\vec{y_i},x)$  are obtained to approximate the solutions of the model

$$-\nabla \cdot (K_N(\vec{y}_i, x) \nabla \phi_N(\vec{y}_i, x)) = f_D, \tag{41}$$

$$-\nabla \cdot \mathbb{T}(\vec{u}_N(\vec{y}_i, x), p_N(\vec{y}_i, x)) = \vec{f}_S, \tag{42}$$

$$\nabla \cdot \vec{u}_N(\vec{y}_i, x) = 0, \tag{43}$$

$$\vec{u}_N(\vec{y}_i, x) \cdot \vec{n}_S = K_N(\vec{y}_i, x) \nabla \phi_N(\vec{y}_i, x) \cdot \vec{n}_D, \tag{44}$$

$$-\vec{n}_S \cdot (\mathbb{T}(\vec{u}_N(\vec{y}_i, x), p_N(\vec{y}_i, x)) \cdot \vec{n}_S) = g(\phi_N(\vec{y}_i, x) - z), \tag{45}$$

$$-\boldsymbol{\tau}_{j}\cdot(\mathbb{T}(\vec{u}_{N}(\vec{y}_{i},x),p_{N}(\vec{y}_{i},x))\cdot\vec{n}_{S})-\boldsymbol{\tau}_{j}\cdot(\mathbb{T}(\vec{u}_{N}(\vec{y}_{i},x),p_{N}(\vec{y}_{i},x))\cdot\vec{n}_{S})$$

$$= \frac{\alpha\nu\sqrt{\mathbf{d}}}{\sqrt{\operatorname{trace}(\prod_{N})}}\boldsymbol{\tau}_{j} \cdot (\vec{u}_{N}(\vec{y}_{i}, x) + K_{N}(\vec{y}_{i}, x)\nabla\phi_{N}(\vec{y}_{i}, x)). \tag{46}$$

3: Return: Calculate the expected value:

$$\mathbb{E}[\phi_N](x) = \sum_{i=1}^M w_i \phi_N(\vec{y}_i, x), \tag{47}$$

$$\mathbb{E}[\vec{u}_N](x) = \sum_{i=1}^M w_i \vec{u}_N(\vec{y}_i, x), \tag{48}$$

$$\mathbb{E}[p_N](x) = \sum_{i=1}^{M} w_i p_N(\vec{y}_i, x). \tag{49}$$

4.3. Numerical algorithm for deterministic Stokes-Darcy model. In order to obtain the finite element solutions  $\phi_{N,h}(\vec{y}_i,x)$ ,  $\vec{u}_{N,h}(\vec{y}_i,x)$  and  $p_{N,h}(\vec{y}_i,x)$  at the second step in Algorithm 1, we recall the finite element method to solve the deterministic Stokes-Darcy model at each collocation node (i.e., for each sample):

$$-\nabla \cdot (K\nabla \phi_D) = f_D, \text{ in } \Omega_D, \tag{50}$$

$$-\nabla \cdot \mathbb{T}(\vec{u}_S, p_S) = \vec{f}_S, \text{ in } \Omega_S, \tag{51}$$

$$\nabla \cdot \vec{u}_S = 0, \text{ in } \Omega_S, \tag{52}$$

$$\vec{u}_S \cdot \vec{n}_S = -\vec{u}_D \cdot \vec{n}_D$$
, on  $\Gamma$ , (53)

$$-\vec{n}_S \cdot (\mathbb{T}(\vec{u}_S, p_S) \cdot \vec{n}_S) = g(\phi_D - z), \text{ on } \Gamma,$$
(54)

$$-\boldsymbol{\tau}_{j} \cdot (\mathbb{T}(\vec{u}_{S}, p_{S}) \cdot \vec{n}_{S}) = \frac{\alpha \nu \sqrt{\mathbf{d}}}{\sqrt{\operatorname{trace}(\prod)}} \boldsymbol{\tau}_{j} \cdot (\vec{u}_{S} - \vec{u}_{D}), \text{ on } \Gamma.$$
 (55)

From the assumptions in Section 2, the hydraulic head  $\phi_D$  and the fluid velocity  $\vec{u}_S$  satisfy homogeneous Dirichlet boundary condition except on  $\Gamma$ , i.e.,  $\phi_D=0$  on the boundary  $\partial\Omega_D\backslash\Gamma$  and  $\vec{u}_S=0$  on the boundary  $\partial\Omega_S\backslash\Gamma$ .

The spaces that we utilize are

$$X_S = \{ \vec{v} \in [H^1(\Omega_S)]^d \mid \vec{v} = 0 \text{ on } \partial \Omega_S \backslash \Gamma \},$$

$$Q_S = L^2(\Omega_S),$$

$$X_D = \{ \psi \in H^1(\Omega_D) \mid \psi = 0 \text{ on } \partial \Omega_D \backslash \Gamma \}.$$

For the domain D ( $D = \Omega_S$  or  $\Omega_D$ ),  $(\cdot, \cdot)_D$  denotes the  $L^2$  inner product on the domain D, and  $\langle \cdot, \cdot \rangle$  denotes the  $L^2$  inner product on the interface  $\Gamma$  or the duality pairing between  $(H_{00}^{1/2}(\Gamma))'$  and  $H_{00}^{1/2}(\Gamma)$ . Let  $P_{\tau}$  denote the projection onto the tangent space on  $\Gamma$ , i.e.,

$$P_{\tau}\vec{u} = \sum_{j=1}^{d-1} (\vec{u} \cdot \boldsymbol{\tau}_j) \boldsymbol{\tau}_j.$$

Define the following bilinear terms.

$$a_D(\phi_D, \psi) = (K\nabla\phi_D, \nabla\psi)_{\Omega_D},$$
  

$$a_S(\vec{u}_S, \vec{v}) = 2\nu(\mathbb{D}(\vec{u}_S), \mathbb{D}(\vec{v}))_{\Omega_S},$$
  

$$b_S(\vec{v}, q) = -(\nabla \cdot \vec{v}, q)_{\Omega_S}.$$

We assume that we have in hand regular subdivisions of  $\Omega_D$  and  $\Omega_S$  into finite elements. Then one can define finite element spaces  $X_{Dh} \subset X_D$ ,  $X_{Sh} \subset X_S$ , and  $Q_{Sh} \subset Q_S$ . We assume that  $X_{Sh}$  and  $Q_{Sh}$  satisfy the inf-sup condition [53,56]

$$\inf_{0 \neq q \in Q_{sh}} \sup_{0 \neq \vec{v} \in X_{Sh}} \frac{b_S(\vec{v}, q)}{\|\vec{v}\|_1 \|q\|_0} > \gamma, \tag{56}$$

where  $\gamma > 0$  is a constant independent of h; this condition is needed to ensure that the spatial discretizations of the Stokes system used here are stable, see [53,56] for details and many examples of pairs of finite element spaces  $X_{Dh}$ ,  $X_{Sh}$ , and  $Q_{Sh}$  that satisfy (56). One typical example is the Taylor-Hood element pair that we use in the numerical experiments; for that pair,  $X_{Dh}$  and  $X_{Sh}$  consist of continuous piecewise quadratic polynomials and  $Q_{Sh}$  consists of continuous piecewise linear polynomials.

Then we recall the finite element formulation of the Stokes-Darcy problem as follows: [25,26]: find  $(\vec{u}_h, p_h) \in X_{Sh} \times Q_{Sh}$  and  $\phi_h \in X_{Sh}$  such that

$$a_{S}(\vec{u}_{h}, \vec{v}_{h}) + b_{S}(\vec{v}_{h}, p_{h}) + a_{D}(\phi_{h}, \psi_{h}) + \langle g\phi_{h}, \vec{v}_{h} \cdot \vec{n}_{S} \rangle$$
$$-\langle \vec{u}_{h} \cdot \vec{n}_{S}, \psi_{h} \rangle + \frac{\alpha \nu \sqrt{\mathbf{d}}}{\sqrt{\operatorname{trace}(\prod)}} \langle P_{\tau}(\vec{u}_{h} + K \nabla \phi_{h}), P_{\tau} \vec{v}_{h} \rangle$$
(57)

$$= (f_D, \psi_h)_{\Omega_D} + (\vec{f}, \vec{v}_h)_{\Omega_S} + \langle gz, \vec{v}_h \cdot \vec{n}_S \rangle, \ \forall \ \vec{v}_h \in X_{Sh}, \ \psi_h \in X_{Dh},$$

$$b_S(\vec{u}_h, q_h) = 0, \quad \forall \ q_h \in Q_{Sh}.$$

$$(58)$$

5. Computational examples. We consider the model problem (3)-(8) on  $\Omega = [0,1] \times [-0.25,0.75]$ , where  $\Omega_D = [0,1] \times [0,0.75]$  and  $\Omega_S = [0,1] \times [-0.25,0]$ . For the physical parameters, we choose  $\frac{\alpha\nu\sqrt{\mathbf{d}}}{\sqrt{\mathrm{trace}(\prod)}} = 1$ ,  $\nu = 1$ , g = 1, and z = 0.

The boundary condition data functions and the source terms are

$$f_{D} = -\pi^{3} \sin(\pi x)(-y + \cos(\pi(1-y))) - (2 - \pi \sin(\pi x))(-\pi^{2} \cos(\pi(1-y))),$$

$$\vec{f}_{S1} = -2\nu x^{2} - 2\nu y^{2} - \nu e^{-y} + \pi^{2} \cos(\pi x) \cos(2\pi y),$$

$$\vec{f}_{S2} = 4\nu xy - \nu \pi^{3} \sin(\pi x) + 2\pi(2 - \pi \sin(\pi x)) \sin(2\pi y),$$

$$\phi_{D} = (2 - \pi \sin(\pi x))(-y + \cos(\pi(1-y))), \text{ on } \partial\Omega_{D} \backslash \Gamma,$$

$$\vec{u}_{S} = (x^{2}y^{2} + e^{-y}, -2xy^{3}/3 + 2 - \pi \sin(\pi x)), \text{ on } \partial\Omega_{S} \backslash \Gamma.$$

For the discrete form in physical space by the finite element method, we use a uniform grid with grid size h=1/32. The Taylor-Hood element pair is used for the Stokes system and the quadratic finite element is used for the primary formulation of the Darcy system.

By the truncated KL expansion, the random hydraulic conductivity  $K(\omega, x)$  is given as [91]

$$\ln(K(\omega, x) - 0.5) = 1 + Z_1(\omega) \left(\frac{\sqrt{\pi}L}{2}\right)^{1/2} + \sum_{n=2}^{N} \zeta_n \phi_n(x) Z_n(\omega), \quad (59)$$

where

$$\zeta_n = \left(\sqrt{\pi}L\right)^{1/2} \exp\left(\frac{-(\lfloor n/2\rfloor \pi L)^2}{8}\right), \quad n > 1,$$
(60)

and

$$\phi_n(x) = \begin{cases} \sin\left(\frac{\lfloor n/2\rfloor\pi x}{L_p}\right), & \text{if } n \text{ is even,} \\ \cos\left(\frac{\lfloor n/2\rfloor\pi x}{L_p}\right), & \text{if } n \text{ is odd.} \end{cases}$$
(61)

Here  $\lfloor \cdot \rfloor$  is the floor function giving as output the greatest integer less than or equal to the input. In this example, the random variables  $\{Z_n(\omega)\}_{n=1}^N$  are independent, and have zero mean and unit variance, i.e.,  $\mathbb{E}[Z_n] = 0$  and  $\mathbb{E}[Z_n Z_m] = \delta_{nm}$  for  $n, m \in N+$ . We assume that the random variables  $\{Z_n(\omega)\}_{n=1}^N$  are uniformly distributed in the interval  $[-\sqrt{3}, \sqrt{3}]$ . Let  $L_c$  be a desired physical correlation length for the coefficient K. Then the parameter  $L_p$  is  $L_p = \max\{1, 2L_c\}$  and the parameter L is  $L = L_c/L_p$ . The decay rate of the eigenvalues  $\lambda_n$  depends on the correlation length  $L_c$ .

For evaluating the accuracy of numerical solutions with different accuracy level s in the sparse grid method, we generate the reference solutions with the mesh size h=1/32 and s=7, when we choose N=5 in the truncated Karhunen-Loève expansion. And the reference solutions are constructed with the mesh size h=1/32 and s=6 when we choose N=10. In the Table 1 and Table 2, the number of sparse grid nodes with different accuracy level s are listed for N=5 and N=10, respectively. It is obvious that significant computational cost can be saved if the cases with smaller s can still provide accurate enough solutions.

Table 1. Number of sparse grid nodes with different accuracy level s when N=5

| $\overline{s}$ | 2  | 3  | 4   | 5   | 6    | 7    |
|----------------|----|----|-----|-----|------|------|
| KPU            | 11 | 51 | 151 | 391 | 903  | 1743 |
| GQU            | 11 | 61 | 241 | 781 | 2203 | 5593 |

Table 2. Number of sparse grid nodes with different accuracy level s when N=10

| s   | 2  | 3   | 4    | 5    | 6     |
|-----|----|-----|------|------|-------|
| KPU | 21 | 201 | 1201 | 5281 | 19105 |
| GQU | 21 | 221 | 1581 | 8761 | 40405 |

We exhibit the convergence of the numerical errors in  $L^2$  norm of the mean value and the variance of the velocity in Figure 2 and Figure 3 with  $L_c = 1/64$ . It is observed that errors in  $L^2$  norm decrease fast as the parameter s increases. Based on this convergence performance to the reference case (s = 7 for N = 5 or s = 6 for N = 10), it is accurate enough to choose smaller s in the sparse grid algorithm to calculate the numerical solutions with much less computational cost.

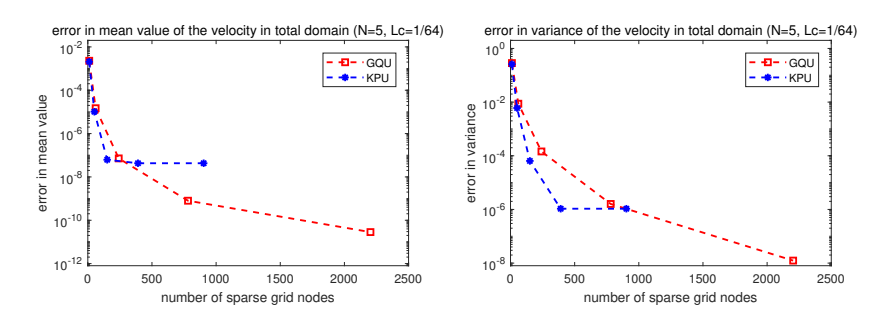


FIGURE 2. The convergence in  $L^2$  norm for the expected value (left) and the variance (right) of velocity with N=5 and  $L_c=1/64$ .

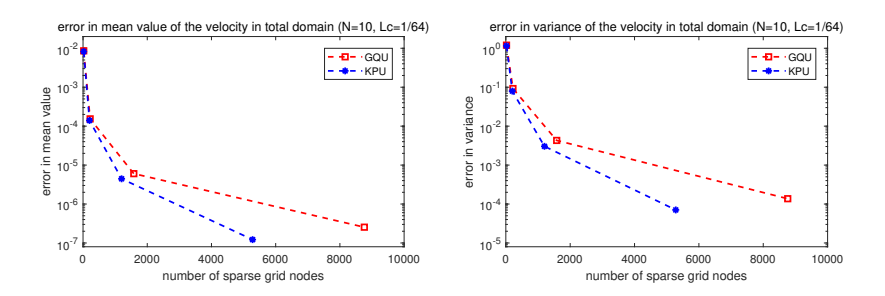


FIGURE 3. The convergence in  $L^2$  norm for the expected value (left) and the variance (right) of velocity with N=10 and  $L_c=1/64$ .

To investigate the influence of correlation length  $L_c$ , we show the convergence of the numerical errors in  $L^2$  norm of the mean value and the variance of the velocity with different correlation lengths  $L_c$  in Figure 4 for N=5 and GQU sparse grid

nodes. As expected, the larger correlation lengths  $L_c$  slow down the convergence. But it is still accurate enough to choose smaller s in the sparse grid algorithm to calculate the numerical solutions with much less computational cost.

In Figure 5, we show the convergence of the numerical errors in  $L^2$  norm of the mean value and the variance of the velocity with different correlation lengths  $L_c$  for N=10 and GQU sparse grid nodes. Similar to the case of N=5, numerical errors in  $L^2$  norm decrease when s becomes larger.

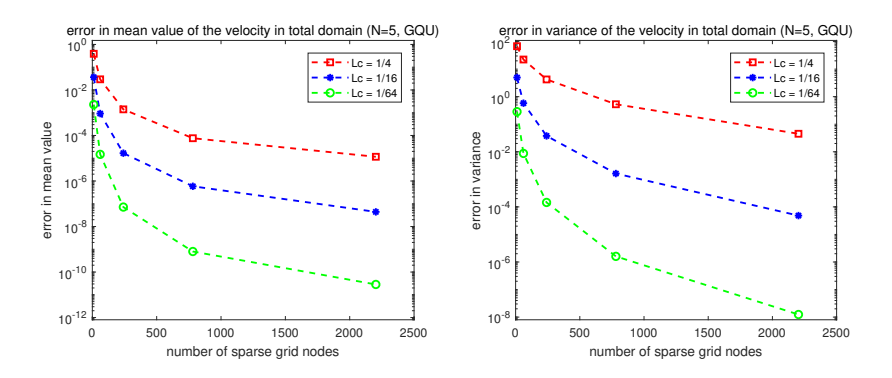


FIGURE 4. The convergence in  $L^2$  norm for the expected value (left) and the variance (right) of velocity with N=5, GQU method, and different correlation length  $L_c$ .

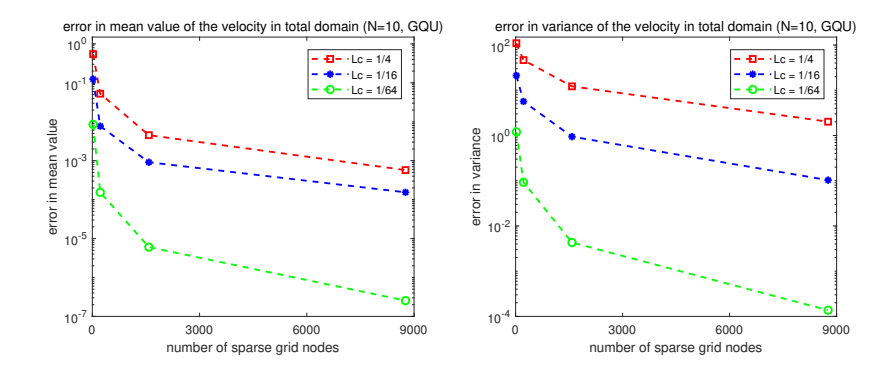


FIGURE 5. The convergence in  $L^2$  norm for the expected value (left) and the variance (right) of velocity with N=10, GQU method, and different correlation length  $L_c$ .

In Figure 6, we pick three samples to illustrate the influence of the random hydraulic conductivity K on the flow field. Even though all the set-up inside the free flow subdomain  $\Omega_S$  is deterministic, it is expected to observe that the randomness is passed from the porous media subdomain  $\Omega_D$  to the free flow subdomain  $\Omega_S$  through the interface conditions which are affected by the randomness in  $\Omega_D$ . To further illustrate the randomness in porous media subdomain  $\Omega_D$  and free flow

subdomain  $\Omega_S$ , we show the variance of the speed in total domain in Figure 7. One can see that the variance of speed in porous media subdomain  $\Omega_D$  is much larger than the variance of speed in free flow subdomain  $\Omega_S$ .

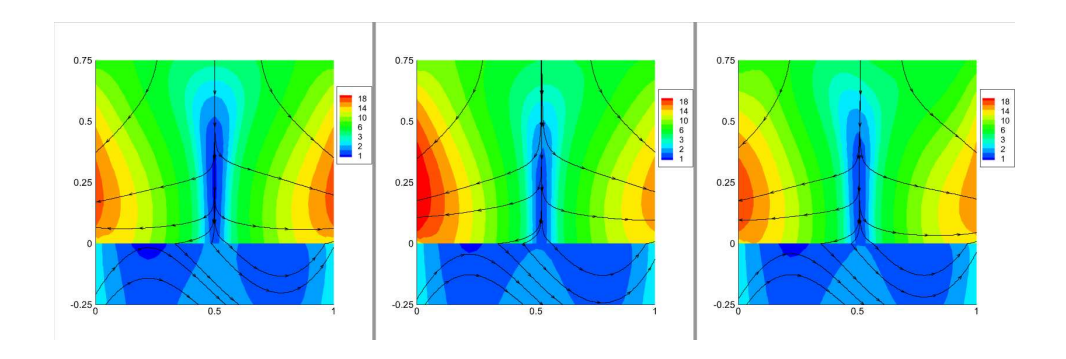


FIGURE 6. Numerical solutions of three samples of GQU with N=10 and s=6. The color represents the speed of flow and the streamlines show the direction of the flow.

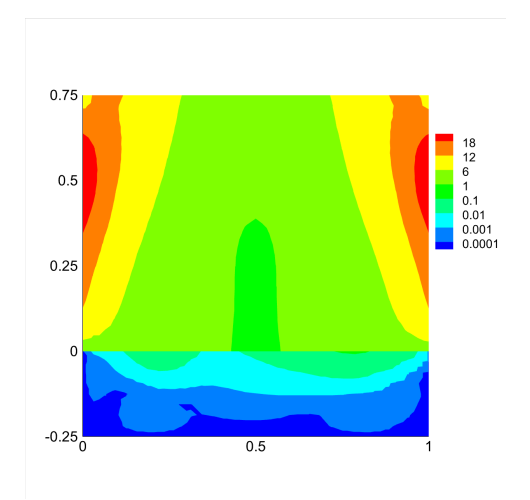


FIGURE 7. Variance of the speed of samples of GQU with N=10 and s=6 in total domain. The color represents the variance of the speed.

6. Conclusions. In this paper we propose a sparse grid stochastic collocation method for a stochastic Stokes-Darcy model with Beavers-Joseph interface condition. Truncated Karhunen-Loève expansion is used to approximate the random field of the hydraulic conductivity. Gauss-Legendre abscissas (GQU) and Kronrod-Patterson abscissas (KPU) are used in the construction of the Smolyak sparse grid formula. The numerical results show that this method is convergent and a small number of sparse grid nodes can be used to calculate the numerical solutions with

enough accuracy and much less computational cost. The influence of the interface conditions on the randomness transmission is also illustrated.

#### REFERENCES

- [1] T. Arbogast and D. S. Brunson, A computational method for approximating a Darcy-Stokes system governing a vuggy porous medium, *Comput. Geosci.*, **11** (2007), 207–218.
- [2] T. Arbogast and M. S. M. Gomez, A discretization and multigrid solver for a Darcy-Stokes system of three dimensional vuggy porous media, Comput. Geosci., 13 (2009), 331–348.
- [3] T. Arbogast and H. L. Lehr, Homogenization of a Darcy-Stokes system modeling vuggy porous media, *Comput. Geosci.*, **10** (2006), 291–302.
- [4] R. Archibald, F. Bao, J. Yong and T. Zhou, An efficient numerical algorithm for solving data driven feedback control problems, J. Sci. Comput., 85 (2020), Paper No. 51, 27 pp.
- [5] M. G. Armentano and M. L. Stockdale, Approximations by mini mixed finite element for the Stokes-Darcy coupled problem on curved domains, Int. J. Numer. Anal. Mod., 18 (2021), 203–234.
- [6] I. Babuška and G. N. Gatica, A residual-based a posteriori error estimator for the Stokes-Darcy coupled problem, SIAM J. Numer. Anal., 48 (2010), 498–523.
- [7] I. Babuška, F. Nobile and R. Tempone, A stochastic collocation method for elliptic partial differential equations with random input data, SIAM Rev., 52 (2010), 317–355.
- [8] I. Babuška, R. Tempone and G. E. Zouraris, Galerkin finite element approximations of stochastic elliptic partial differential equations, SIAM J. Numer. Anal., 42 (2004), 800–825.
- [9] M. Baccouch, A finite difference method for stochastic nonlinear second-order boundary-value problems driven by additive noises, Int. J. Numer. Anal. Mod., 17 (2020), 368–389.
- [10] L. Badea, M. Discacciati and A. Quarteroni, Numerical analysis of the Navier-Stokes/Darcy coupling, Numer. Math., 115 (2010), 195–227.
- [11] F. Bao, Y. Cao, C. Webster and G. Zhang, A hybrid sparse-grid approach for nonlinear filtering problems based on adaptive-domain of the Zakai equation approximations, SIAM/ASA J. Uncertain. Quantif., 2 (2014), 784–804.
- [12] F. Bao and V. Maroulas, Adaptive meshfree backward SDE filter, SIAM J. Sci. Comput., 39 (2017), A2664–A2683.
- [13] G. Bao, Y. Cao, J. Lin and H. W. van Wyk, Computational optimal design of random rough surfaces in thin-film solar cells, Commun. Comput. Phys., 25 (2019), 1591–1612.
- [14] A. Barth, C. Schwab and N. Zollinger, Multi-level Monte Carlo finite element method for elliptic PDEs with stochastic coefficients, Numer. Math., 119 (2011), 123–161.
- [15] V. Barthelmann, E. Novak and K. Ritter, High dimensional polynomial interpolation on sparse grids, Adv. Comput. Math., 12 (2000), 273–288.
- [16] G. S. Beavers and D. D. Joseph, Boundary conditions at a naturally permeable wall, J. Fluid Mech., 30 (1967), 197–207.
- [17] C. Bernardi, T. C. Rebollo, F. Hecht and Z. Mghazli, Mortar finite element discretization of a model coupling Darcy and Stokes equations, M2AN Math. Model. Numer. Anal., 42 (2008), 375–410.
- [18] Y. Boubendir and S. Tlupova, Stokes-Darcy boundary integral solutions using preconditioners, J. Comput. Phys., 228 (2009), 8627–8641.
- [19] Y. Boubendir and S. Tlupova, Domain decomposition methods for solving Stokes-Darcy problems with boundary integrals, SIAM J. Sci. Comput., 35 (2013), B82–B106.
- [20] M. Cai, M. Mu, and J. Xu, Numerical solution to a mixed Navier-Stokes/Darcy model by the two-grid approach, SIAM J. Numer. Anal., 47 (2009), 3325–3338.
- [21] J. Camano, G. N. Gatica, R. Oyarzua, R. Ruiz-Baier and P. Venegas, New fully-mixed finite element methods for the Stokes-Darcy coupling, Comput. Methods Appl. Mech. Engrg., 295 (2015), 362–395.
- [22] Y. Cao, Y. Chu, X. He and M. Wei, Decoupling the stationary Navier-Stokes-Darcy system with the Beavers-Joseph-Saffman interface condition, Abstr. Appl. Anal., (2013), pages Article ID 136483, 10 pp.
- [23] Y. Cao, M. Gunzburger, X. He and X. Wang, Robin-Robin domain decomposition methods for the steady Stokes-Darcy model with Beaver-Joseph interface condition, *Numer. Math.*, 117 (2011), 601–629.

- [24] Y. Cao, M. Gunzburger, X. He and X. Wang, Parallel, non-iterative, multi-physics domain decomposition methods for time-dependent Stokes-Darcy systems, Math. Comp., 83 (2014), 1617–1644.
- [25] Y. Cao, M. Gunzburger, X. Hu, F. Hua, X. Wang and W. Zhao, Finite element approximation for Stokes-Darcy flow with Beavers-Joseph interface conditions, SIAM. J. Numer. Anal., 47 (2010), 4239–4256.
- [26] Y. Cao, M. Gunzburger, F. Hua and X. Wang, Coupled Stokes-Darcy model with Beavers-Joseph interface boundary condition, Comm. Math. Sci., 8 (2010), 1–25.
- [27] Y. Cao, J. Hong and Z. Liu, Approximating stochastic evolution equations with additive white and rough noises, SIAM J. Numer. Anal., 55 (2017), 1958–1981.
- [28] A. Çeşmelioğlu and B. Rivière, Primal discontinuous Galerkin methods for time-dependent coupled surface and subsurface flow, J. Sci. Comput., 40 (2009), 115–140.
- [29] J. Charrier, R. Scheichl and A. L. Teckentrup, Finite element error analysis of elliptic PDEs with random Coefficients and its application to multilevel Monte Carlo methods, SIAM J. Numer. Anal., 51 (2013), 322–352.
- [30] N. Chen, M. Gunzburger and X. Wang, Asymptotic analysis of the differences between the Stokes-Darcy system with different interface conditions and the Stokes-Brinkman system, J. Math. Anal. Appl., 368 (2010), 658–676.
- [31] W. Chen, M. Gunzburger, F. Hua and X. Wang, A parallel Robin-Robin domain decomposition method for the Stokes-Darcy system, SIAM. J. Numer. Anal., 49 (2011), 1064–1084.
- [32] W. Chen, M. Gunzburger, D. Sun and X. Wang, Efficient and long-time accurate second-order methods for the Stokes-Darcy system, SIAM J. Numer. Anal., 51 (2013), 2563–2584.
- [33] P. Chidyagwai and B. Rivière, On the solution of the coupled Navier-Stokes and Darcy equations, Comput. Methods Appl. Mech. Engrg., 198 (2009), 3806–3820.
- [34] Y. Choi and H.-C. Lee, Error analysis of finite element approximations of the optimal control problem for stochastic Stokes equations with additive white noise, *Appl. Numer. Math.*, **133** (2018), 144–160.
- [35] M. K. Deb, I. M. Babuška, and J. T. Oden, Solution of stochastic partial differential equations using galerkin finite element techniques, Comput. Methods Appl. Mech. Engrg., 190 (2001), 6359–6372.
- [36] M. Discacciati, Domain Decomposition Methods for the Coupling of Surface and Groundwater Flows, PhD thesis, Ecole Polytechnique Fédérale de Lausanne, Switzerland, 2004.
- [37] M. Discacciati and L. Gerardo-Giorda, Optimized Schwarz methods for the Stokes-Darcy coupling, IMA J. Numer. Anal., 38 (2018), 1959–1983.
- [38] M. Discacciati, E. Miglio and A. Quarteroni, Mathematical and numerical models for coupling surface and groundwater flows, Appl. Numer. Math., 43 (2002), 57–74.
- [39] M. Discacciati and A. Quarteroni, Convergence analysis of a subdomain iterative method for the finite element approximation of the coupling of Stokes and Darcy equations, Comput. Vis. Sci., 6 (2004), 93–103.
- [40] M. Discacciati, A. Quarteroni and A. Valli, Robin-Robin domain decomposition methods for the Stokes-Darcy coupling, SIAM J. Numer. Anal., 45 (2007), 1246–1268.
- [41] C. Douglas, X. Hu, B. Bai, X. He, M. Wei and J. Hou, A data assimilation enabled model for coupling dual porosity flow with free flow, 17th International Symposium on Distributed Computing and Applications for Business Engineering and Science (DCABES), Wuxi, China, (2018), 304–307.
- [42] D. Drzisga, B. Gmeiner, U. Rüde, R. Scheichl and B. Wohlmuth, Scheduling massively parallel multigrid for multilevel Monte Carlo methods, SIAM J. Sci. Comput., 39 (2017), S873–S897.
- [43] V. J. Ervin, E. W. Jenkins and H. Lee, Approximation of the Stokes-Darcy system by optimization, J. Sci. Comput., 59 (2014), 775–794.
- [44] V. J. Ervin, E. W. Jenkins and S. Sun, Coupled generalized nonlinear Stokes flow with flow through a porous medium, SIAM J. Numer. Anal., 47 (2009), 929–952.
- [45] W. Feng, X. He, Z. Wang and X. Zhang, Non-iterative domain decomposition methods for a non-stationary Stokes-Darcy model with Beavers-Joseph interface condition, Appl. Math. Comput., 219 (2012), 453–463.
- [46] G. S. Fishman, Monte Carlo: Concepts, Algorithms, and Applications, Springer Ser. Oper. Res. Springer-Verlag, New York, 1996.
- [47] P. Frauenfelder, C. Schwab and R. A. Todor, Finite elements for elliptic problems with stochastic coefficients, Comput. Methods Appl. Mech. Engrg., 194 (2005), 205–228.

- [48] J. Galvis and M. Sarkis, Non-matching mortar discretization analysis for the coupling Stokes-Darcy equations, Electron. Trans. Numer. Anal., 26 (2007), 350–384.
- [49] Y. Gao, X. He, L. Mei and X. Yang, Decoupled, linear, and energy stable finite element method for the Cahn-Hilliard-Navier-Stokes-Darcy phase field model, SIAM J. Sci. Comput., 40 (2018), B110–B137.
- [50] G. N. Gatica, S. Meddahi and R. Oyarzúa, A conforming mixed finite-element method for the coupling of fluid flow with porous media flow, IMA J. Numer. Anal., 29 (2009), 86–108.
- [51] T. Gerstner and M. Griebel, Numerical integration using sparse grids, Numer. Algorithms, 18 (1998), 209–232.
- [52] M. Giles, Improved multilevel Monte Carlo convergence using the Milstein scheme, In Monte Carlo and Quasi-Monte Carlo Methods 2006, Springer, (2008), 343–358.
- [53] V. Girault and P.-A. Raviart, Finite Element Methods for Navier-Stokes Equations. Theory and Algorithms, volume 5 of Springer Series in Computational Mathematics, Springer-Verlag, Berlin, 1986.
- [54] V. Girault and B. Rivière, DG approximation of coupled Navier-Stokes and Darcy equations by Beaver-Joseph-Saffman interface condition, SIAM J. Numer. Anal, 47 (2009), 2052–2089.
- [55] V. Girault, D. Vassilev and I. Yotov, Mortar multiscale finite element methods for Stokes-Darcy flows, Numer. Math., 127 (2014), 93–165.
- [56] M. D. Gunzburger, Finite Element Methods for Viscous Incompressible Flows. A Guide to Theory, Practice, and Algorithms, Computer Science and Scientific Computing. Academic Press, Boston, MA, 1989.
- [57] M. Gunzburger, X. He and B. Li, On Ritz projection and multi-step backward differentiation schemes in decoupling the Stokes-Darcy model, SIAM J. Numer. Anal., 56 (2018), 397–427.
- [58] M. D. Gunzburger, H.-C. Lee and J. Lee, Error estimates of stochastic optimal Neumann boundary control problems, SIAM J. Numer. Anal., 49 (2011), 1532–1552.
- [59] L. Guo, A. Narayan, T. Zhou and Y. Chen, Stochastic collocation methods via l<sub>1</sub> minimization using randomized quadratures, SIAM J. Sci. Comput., 39 (2017), A333–A359.
- [60] D. Han, X. He, Q. Wang, and Y. Wu, Existence and weak-strong uniqueness of solutions to the Cahn-Hilliard-Navier-Stokes-Darcy system in superposed free flow and porous media, Nonlinear Anal., 211 (2021), Paper No. 112411, 27 pp.
- [61] D. Han, D. Sun and X. Wang, Two-phase flows in karstic geometry, Math. Methods Appl. Sci., 37 (2014), 3048–3063.
- [62] N. S. Hanspal, A. N. Waghode, V. Nassehi and R. J. Wakeman, Numerical analysis of coupled Stokes/Darcy flow in industrial filtrations, Transp. Porous Media, 64 (2006), 73–101.
- [63] X. He, N. Jiang and C. Qiu, An artificial compressibility ensemble algorithm for a stochastic Stokes-Darcy model with random hydraulic conductivity and interface conditions, Int. J. Numer. Meth. Eng., 121 (2020), 712–739.
- [64] X. He, J. Li, Y. Lin and J. Ming, A domain decomposition method for the steady-state Navier-Stokes-Darcy model with Beavers-Joseph interface condition, SIAM J. Sci. Comput., 37 (2015), S264–S290.
- [65] F. Heiss and V. Winschel, Likelihood approximation by numerical integration on sparse grids, J. Econometrics, 144 (2008), 62–80.
- [66] R. H. W. Hoppe, P. Porta and Y. Vassilevski, Computational issues related to iterative coupling of subsurface and channel flows, Calcolo, 44 (2007), 1–20.
- [67] J. Hou, M. Qiu, X. He, C. Guo, M. Wei and B. Bai, A dual-porosity-Stokes model and finite element method for coupling dual-porosity flow and free flow, SIAM J. Sci. Comput., 38 (2016), B710–B739.
- [68] I. Igreja and A. F. D. Loula, A stabilized hybrid mixed DGFEM naturally coupling Stokes-Darcy flows, Comput. Methods Appl. Mech. Engrg., 339 (2018), 739–768.
- [69] J. D. Jakeman, A. Narayan and T. Zhou, A generalized sampling and preconditioning scheme for sparse approximation of polynomial chaos expansions, SIAM J. Sci. Comput., 39 (2017), A1114–A1144.
- [70] N. Jiang and C. Qiu, An efficient ensemble algorithm for numerical approximation of stochastic Stokes-Darcy equations, Comput. Methods Appl. Mech. Engrg., 343 (2019), 249–275.
- [71] G. Kanschat and B. Riviére, A strongly conservative finite element method for the coupling of Stokes and Darcy flow, J. Comput. Phys., 229 (2010), 5933–5943.
- [72] T. Karper, K.-A. Mardal and R. Winther, Unified finite element discretizations of coupled Darcy-Stokes flow, Numer. Methods Partial Differential Equations, 25 (2009), 311–326.

- [73] R. Kornhuber, C. Schwab and M.-W. Wolf, Multilevel Monte Carlo finite element methods for stochastic elliptic variational inequalities, SIAM J. Numer. Anal., 52 (2014), 1243–1268.
- [74] P. Kumara, P. Luo, F. J. Gaspara and C. W. Oosterleea, A multigrid multilevel Monte Carlo method for transport in the Darcy-Stokes system, J. Comput. Phys., 371 (2018), 382–408.
- [75] W. Layton, H. Tran and C. Trenchea, Analysis of long time stability and errors of two partitioned methods for uncoupling evolutionary groundwater-surface water flows, SIAM J. Numer. Anal., 51 (2013), 248–272.
- [76] W. J. Layton, F. Schieweck and I. Yotov, Coupling fluid flow with porous media flow, SIAM J. Numer. Anal., 40 (2002), 2195–2218.
- [77] R. Li, J. Li, X. He and Z. Chen, A stabilized finite volume element method for a coupled Stokes-Darcy problem, *Appl. Numer. Math.*, **133** (2018), 2–24.
- [78] K. Lipnikov, D. Vassilev and I. Yotov, Discontinuous Galerkin and mimetic finite difference methods for coupled Stokes-Darcy flows on polygonal and polyhedral grids, *Numer. Math.*, 126 (2014), 321–360.
- [79] Y. Liu, Y. He, X. Li and X. He, A novel convergence analysis of Robin-Robin domain decomposition method for Stokes-Darcy system with Beavers-Joseph interface condition, Appl. Math. Lett., 119 (2021), Paper No. 107181, 9 pp.
- [80] M. Loève, Probability Theory, I, volume 45 of Grad. Texts in Math., Springer-Verlag, New York, 4th edition edition, 1977.
- [81] M. Loève, Probability Theory, II, volume 46 of Grad. Texts in Math., Springer-Verlag, New York, 4th edition edition, 1978.
- [82] J. Lyu, Z. Wang, J. Xin and Z. Zhang, Convergence analysis of stochastic structurepreserving schemes for computing effective diffusivity in random flows, SIAM J. Numer. Anal., 58 (2020), 3040–3067.
- [83] Md. A. Al Mahbub, X. He, N. J. Nasu, C. Qiu, Y. Wang and H. Zheng, A coupled multiphysics model and a decoupled stabilized finite element method for closed-loop geothermal system, SIAM J. Sci. Comput., 42 (2020), B951–B982.
- [84] Md. A. Al Mahbub, X. He, N. J. Nasu, C. Qiu and H. Zheng, Coupled and decoupled stabilized mixed finite element methods for non-stationary dual-porosity-Stokes fluid flow model, Int. J. Numer. Meth. Eng., 120 (2019), 803–833.
- [85] A. Márquez, S. Meddahi and F.-J. Sayas, Strong coupling of finite element methods for the Stokes-Darcy problem, IMA J. Numer. Anal., 35 (2015), 969–988.
- [86] H. G. Matthies and A. Keese, Galerkin methods for linear and nonlinear elliptic stochastic partial differential equations, Comput. Methods Appl. Mech. Engrg., 194 (2005), 1295–1331.
- [87] Z. Morrow and M. Stoyanov, A method for dimensionally adaptive sparse trigonometric interpolation of periodic functions, SIAM J. Sci. Comput., 42 (2020), A2436–A2460.
- [88] M. Mu and J. Xu, A two-grid method of a mixed Stokes-Darcy model for coupling fluid flow with porous media flow, SIAM J. Numer. Anal., 45 (2007), 1801–1813.
- [89] S. Münzenmaier and G. Starke, First-order system least squares for coupled Stokes-Darcy flow, SIAM J. Numer. Anal., 49 (2011), 387–404.
- [90] F. Nobile, R. Tempone and C. G. Webster, An anisotropic sparse grid stochastic collocation method for partial differential equations with random input data, SIAM J. Numer. Anal., 46 (2008), 2411–2442.
- [91] F. Nobile, R. Tempone and C. G. Webster, A sparse grid stochastic collocation method for partial differential equations with random input data, SIAM J. Numer. Anal., 46 (2008), 2309–2345.
- [92] T. N. L. Patterson, The optimum addition of points to quadrature formulae, Math. Comp., 22 (1968), 847–856.
- [93] K. Petras, Smolyak cubature of given polynomial degree with few nodes for increasing dimension, Numer. Math., 93 (2003), 729–753.
- [94] R. Piessens and M. Branders, A note on the optimal addition of abscissas to quadrature formulas of Gauss and Lobatto type, Math. Comp., 28 (1974), 135–139.
- [95] C. Qiu, X. He, J. Li and Y. Lin, A domain decomposition method for the time-dependent Navier-Stokes-Darcy model with Beavers-Joseph interface condition and defective boundary condition, J. Comput. Phys., 411 (2020), 109400, 25 pp.
- [96] B. Rivière and I. Yotov, Locally conservative coupling of Stokes and Darcy flows, SIAM J. Numer. Anal., 42 (2005), 1959–1977.
- [97] P. Robbe, D. Nuyens and S. Vandewalle, Recycling samples in the multigrid multilevel (quasi-)Monte Carlo method, SIAM J. Sci. Comput., 41 (2019), S37–S60.

- [98] L. J. Roman and M. Sarkis, Stochastic galerkin method for elliptic SPDEs: A white noise approach, Discrete Contin. Dyn. Syst. Ser. B, 6 (2006), 941–955.
- [99] H. Rui and R. Zhang, A unified stabilized mixed finite element method for coupling Stokes and Darcy flows, Comput. Methods Appl. Mech. Engrg., 198 (2009), 2692–2699.
- [100] I. Rybak and J. Magiera, A multiple-time-step technique for coupled free flow and porous medium systems, J. Comput. Phys., 272 (2014), 327–342.
- [101] L. Shan and H. Zheng, Partitioned time stepping method for fully evolutionary Stokes-Darcy flow with Beavers-Joseph interface conditions, SIAM J. Numer. Anal., 51 (2013), 813–839.
- [102] S. A. Smolyak, Quadrature and interpolation formulas for tensor products of certain classes of functions, Dokl. Akad. Nauk SSSR, 148 (1963), 1042–1045.
- [103] A. Tambue and J. D. Mukam, Strong convergence and stability of the semi-tamed and tamed euler schemes for stochastic differential equations with jumps under non-global lipschitz condition, Int. J. Numer. Anal. Mod., 16 (2019), 847–872.
- [104] A. L. Teckentrup, R. Scheichl, M. B. Giles and E. Ullmann, Further analysis of multilevel monte carlo methods for elliptic PDEs with random coefficients, *Numer. Math.*, 125 (2013), 569–600.
- [105] H. Tiesler, R. M. Kirby, D. Xiu and T. Preusser, Stochastic collocation for optimal control problems with stochastic PDE constraints, SIAM J. Control Optim., 50 (2012), 2659–2682.
- [106] R. A. Todor, Sparse Perturbation Algorithms for Elliptic Pdeis with Stochastic Data, Ph. D. dissertation, ETH Zurich, Switzerland, 2005.
- [107] H.-W. van Wyk, M. Gunzburger, J. Burkhardt and M. Stoyanov, Power-law noises over general spatial domains and on nonstandard meshes, SIAM/ASA J. Uncertain. Quantif., 3 (2015), 296–319.
- [108] D. Vassilev, C. Wang and I. Yotov, Domain decomposition for coupled Stokes and Darcy flows, Comput. Methods Appl. Mech. Engrg., 268 (2014), 264–283.
- [109] D. Wang, Y. Cao, Q. Li and J. Shen, A stochastic gradient descent method for the design of optimal random interface in thin-film solar cells, *Int. J. Numer. Anal. Mod.*, 18 (2021), 384–398.
- [110] G. Wang, F. Wang, L. Chen and Y. He, A divergence free weak virtual element method for the Stokes-Darcy problem on general meshes, Comput. Methods Appl. Mech. Engrg., 344 (2019), 998–1020.
- [111] W. Wang and C. Xu, Spectral methods based on new formulations for coupled Stokes and Darcy equations, J. Comput. Phys., 257 (2014), part A: 126–142.
- [112] Z. Wang, J. Xin, and Z. Zhang, Computing effective diffusivity of chaotic and stochastic flows using structure-preserving schemes, SIAM J. Numer. Anal., 56 (2018), 2322–2344.
- [113] G. W. Wasilkowski and H. Woźniakowski, Explicit cost bounds of algorithms for multivariate tensor product problems, J. Complexity, 11 (1995), 1–56.
- [114] X. Wei, J. Zhao, X.-M. He, Z. Hu, X. Du and D. Han, Adaptive Kriging method for uncertainty quantification of the photoelectron sheath and dust levitation on the lunar surface, J. Verif. Valid. Uncert., 6 (2021), 011006.
- [115] K. Wu, H. Tang and D. Xiu, A stochastic Galerkin method for first-order quasilinear hyperbolic systems with uncertainty, J. Comput. Phys., 345 (2017), 224–244.
- [116] D. Xiu and G. E. Karniadakis, Modeling uncertainty in steady state diffusion problems via generalized polynomial chaos, Comput. Methods Appl. Mech. Engrg., 191 (2002), 4927–4948.
- [117] D. Xiu and G. E. Karniadakis, The Wiener-Askey polynomial chaos for stochastic differential equations, SIAM J. Sci. Comput., 24 (2002), 619–644.
- [118] D. Zhang, L. Guo and G. E. Karniadakis, Learning in modal space: Solving time-dependent stochastic PDEs using physics-informed neural networks, SIAM J. Sci. Comput., 42 (2020), A639–A665.
- [119] J. Zhang, H. Rui and Y. Cao, A partitioned method with different time steps for coupled Stokes and Darcy flows with transport, Int. J. Numer. Anal. Mod., 16 (2019), 463–498.
- [120] Y. Zhang, C. Zhou, C. Qu, M. Wei, X. He and B. Bai, Fabrication and verification of a glass-silicon-glass micro-nanofluidic model for investigating multi-phase flow in unconventional dual-porosity porous media, Lab Chip, 19 (2019), 4071–4082.
- [121] Z. Zhang, B. Rozovskii and G. E. Karniadakis, Strong and weak convergence order of finite element methods for stochastic PDEs with spatial white noise, Numer. Math., 134 (2016), 61–89

[122] J. Zhao, X. Wei, Z. Hu, X. He and D. Han, Photoelectron sheath near the lunar surface: Fully kinetic modeling and uncertainty quantification analysis, #AIAA 2020-1548, Proceeding of AIAA Scitech 2020 Forum, Orlando, Florida, January 6-10, 2020.

Received March 2021; revised July 2021; early access September 2021.

E-mail address: yangzhp@csrc.ac.cn
E-mail address: xlcdt@mst.edu
E-mail address: hex@mst.edu
E-mail address: jming@hust.edu.cn